

Estimating geohydraulic parameters, protective strength, and corrosivity of hydrogeological units: a case study of ALSCON, Ikot Abasi, southern Nigeria

Jewel I. Ibanga¹ · Nyakno J. George¹

Received: 25 August 2015 / Accepted: 12 February 2016 / Published online: 26 April 2016
© Saudi Society for Geosciences 2016

Abstract The study area, characterized by prolific surface and groundwater repositories, is faced with the challenges of surface and groundwater pollutions. These pollutions need good management practices to avoid waterborne diseases. In an attempt to solve this problem, the integration of vertical electrical sounding (VES) method with laboratory analysis of borehole water was undertaken to size up the contour of groundwater geohydraulic parameter distributions and their dispositions. These Parameters are fraught with information concerning contaminant plume. Aquifer repositories characterized by fine to coarse sands have resistivity ranging from 166.3–2332.5 Ωm , delineated through the use of manual and electronic processing aided by software packages such as WINRESIST and SURFER. Thickness ranged from 2.6–170.3 m. Using the VES results and water resistivity, porosities were determined using Archie's model. Estimated porosities were employed in the Kozeny–Carman–Bear's Model to estimate the hydraulic conductivity for all the VES stations and good fits were obtained with pump test results. The K values were combined with Dar

Zarrouk parameters to infer the hydraulic transmissivity. The results indicate that fractional porosity varies from 0.102 to 0.198. The hydraulic conductivities ranged from 7.48×10^{-6} to 5.33×10^{-5} m/s, while the transmissivity values vary between 7.938×10^{-5} and 3.389×10^{-3} m²/s. The tortuosity of the aquifer also varies from 1.12 to 1.35 while the conductance of aquifer per day varies from 259 to 15,575 $\mu S/day$. The hydrogeological units are generally prone to interaction with brackish/saline water from the Imo River and corrosion from surface sources due to the high permeability of the layers surrounding the geometries of water repositories. The ranges of parameters estimated are consistent with literatures for studies conducted in other areas with similar geomaterials, therefore indicating the efficacy of the method.

Keywords Hydrogeological units · VES · Hydraulic properties · Protective strength · Corrosivity

Introduction

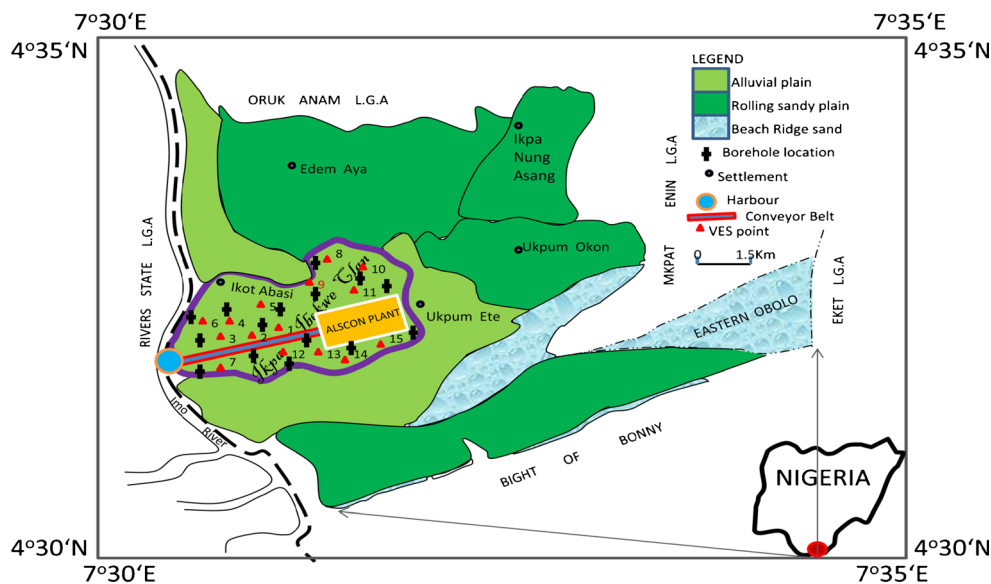
Wildcat exploitation of groundwater is commonly associated with coastal regions, which usually have shallow hydrogeological units. Due to the shallowness of saturated hydrological units in the coastal regions, settlers that care for potable groundwater in an attempt to save money drill without any geophysical information (Ekwe et al. 2006; George et al. 2013). Many settlers ignore the advantages of using potable groundwater and rely on surface water, which is considered by them to be cheap and readily available

✉ Nyakno J. George
nyaknojimmyg@gmail.com

Jewel I. Ibanga
jewelbils@yahoo.com

¹ Department of Physics (Geophysics Research Group), Akwa Ibom State University, Ikot Akpaden, Nigeria

Fig. 1 Maps showing study area, schematic local geological profile of the study area, VES points and borehole locations



(Ibuot et al. 2013; Obianwu et al. 2011a). The method leads to extraction of groundwater from contaminated subsurface hydrological units or from units that suffer high drawdown during dry season as graphic information regarding the quality, quantity, and depth of groundwater available in water repositories are not considered in locating the best and economic hydrological units (Soupios et al. 2007; Obinawu et al. 2011b; Akpan et al. 2013). The ease of groundwater contamination depends on permeability, porosity, overburden thickness of geologic formations, and the geologic divides within the system of hydrogeological units (George et al. 2015a, b). When the underlying geologic material is unconsolidated/uncompacted, such as gravelly or coarse sand, the polluting influents are capable of escaping into the interconnected pores of the subsurface to contaminate hydrologic units, rendering the soil corrosive and forming a polluting plume that extends hundreds of meters (Keswick et al. 1982; George et al. 2014a, b).

Knowledge of water-transmitting properties of a hydrological unit is paramount for successful groundwater development and effective management practices in an area (George et al. 2015a). In this study, the estimation of aquifer geohydraulic parameters at Aluminium Smelter Company of Nigeria (ALSCON) and its adjoining environs from integration of field and laboratory data was carried out using 15 vertical electrical sounding data (VES) and water samples. The result provides the information about the characteristics of the hydrological units and the zones where saltwater from the Imo River interact with the freshwater in the hydrogeological units.

Water tapped from contaminated sources results in the outbreaks of some waterborne diseases such as diarrhea, cholera, guinea worm, bilharziasis, typhoid, etc.

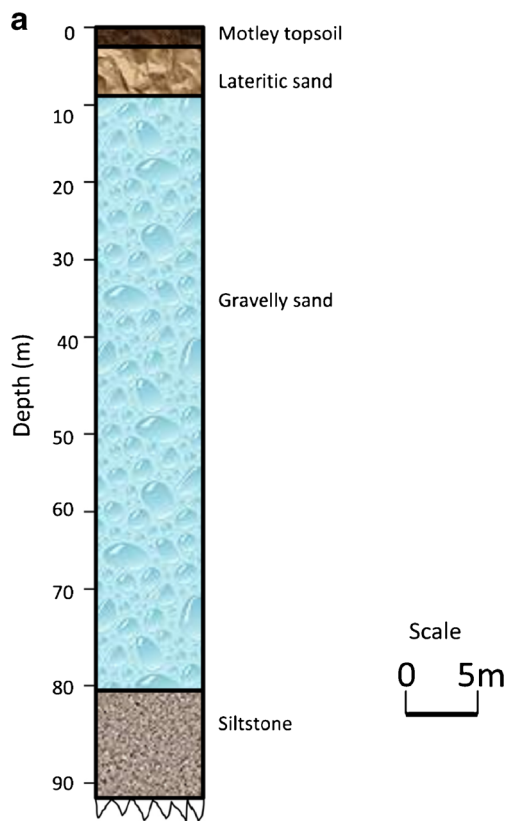


Fig. 2 a A typical water borehole drilled near VES 9 in the study area. b Typical VES representative curves showing VES 1, 2, 7, and 9 in the study area

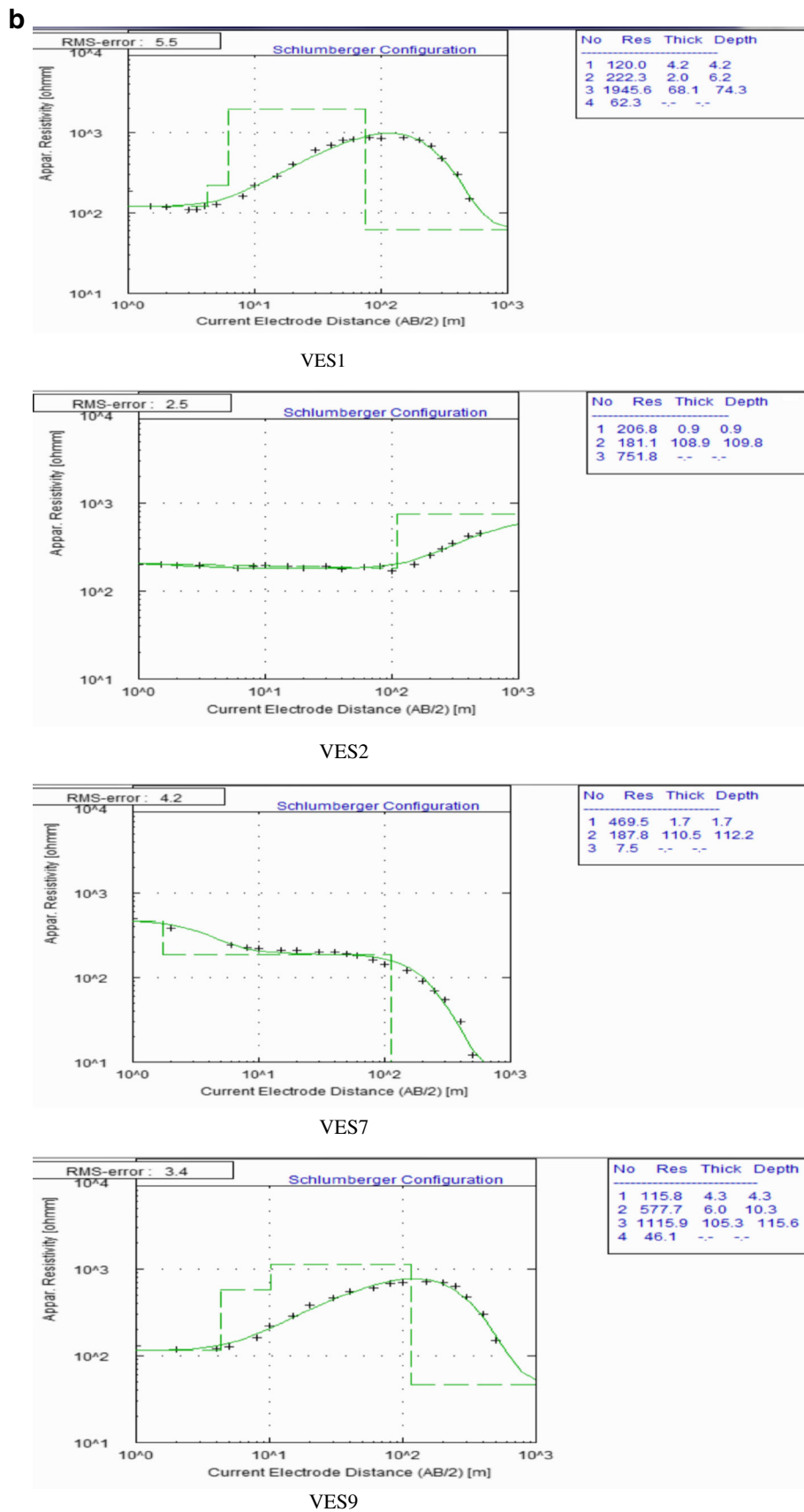


Fig. 2 (continued)

Table 1 Summary of results of geoelectric survey from computer modeling

| VES | Coordinate Lat. (degree) Long. (degree) | Elevation (m) | Layer no. | Layer resistivity (Ωm) | | | | Layer thickness (m) | | | Layer depth (m) | | | Curve type |
|-----|---|---------------|-----------|----------------------------------|----------|----------|----------|---------------------|-------|-------|-----------------|-------|-------|------------|
| | | | | ρ_1 | ρ_2 | ρ_3 | ρ_4 | h_1 | h_2 | h_3 | d_1 | d_2 | d_3 | |
| 1 | 4.56539 N 7.56056 E | 20.0 | 4 | 120.0 | 223.3 | 1945.6 | 62.3 | 4.2 | 2.0 | 68.1 | 4.2 | 6.2 | 74.3 | AK |
| 2 | 4.56644 N 7.56147 E | 16.0 | 3 | 206.8 | 181.1 | 751.8 | – | 0.9 | 108.1 | – | 0.9 | 109.8 | – | H |
| 3 | 4.56431 N 7.56081 E | 12.0 | 3 | 873.2 | 71.3 | 2332.5 | – | 5.1 | 81.1 | – | 5.1 | 86.2 | – | H |
| 4 | 4.56572 N 7.55981 E | 10.0 | 3 | 1020.6 | 735.5 | 1465.9 | – | 7.6 | 87.7 | – | 7.6 | 95.3 | – | H |
| 5 | 4.56702 N 7.55713 E | 10.0 | 4 | 71.8 | 431.8 | 165.5 | 2858.3 | 0.5 | 6.3 | 43.3 | 0.5 | 6.8 | 50.1 | KH |
| 6 | 4.56594 N 7.55675 E | 11.0 | 3 | 554.2 | 362.2 | 1888.4 | – | 11.3 | 170.4 | – | 11.3 | 181.7 | – | H |
| 7 | 4.56322 N 7.56177 E | 12.0 | 3 | 469.5 | 187.8 | 7.5 | – | 1.7 | 110.5 | – | 1.7 | 112.2 | – | Q |
| 8 | 4.66768 N 7.56567 E | 15.0 | 3 | 392.5 | 197.7 | 74.9 | – | 2.4 | 51.9 | – | 2.4 | 54.2 | – | Q |
| 9 | 4.56237 N 7.56322 E | 13.0 | 4 | 115.8 | 577.7 | 1115.9 | 46.1 | 4.3 | 6.0 | 105.3 | 4.3 | 10.3 | 115.6 | AK |
| 10 | 4.67754 N 7.56965 E | 14.0 | 3 | 403.5 | 203.8 | 127.8 | – | 1.4 | 30.9 | – | 1.4 | 32.3 | – | Q |
| 11 | 4.55634 N 7.56786 E | 13.0 | 4 | 90.5 | 396.7 | 8.2 | 25.3 | 1.0 | 5.4 | 94.5 | 1.0 | 6.4 | 100.9 | KH |
| 12 | 4.56566 N 7.56656 E | 14.0 | 4 | 660.4 | 1488.6 | 549.2 | 1248.7 | 1.3 | 3.6 | 47.8 | 1.3 | 4.9 | 52.7 | KH |
| 13 | 4.56452 N 7.56023 E | 15.0 | 4 | 205.8 | 750.3 | 52.6 | 66.8 | 2.9 | 11.8 | 66.2 | 2.9 | 14.7 | 82.9 | KH |
| 14 | 4.55867 N 7.56734 E | 13.0 | 4 | 210.7 | 397.9 | 1721.4 | 228.2 | 0.7 | 12.8 | 55.2 | 0.7 | 13.5 | 68.2 | AK |
| 15 | 4.55945 N 7.56776 E | 14.0 | 4 | 136.4 | 809.6 | 24.2 | 166.3 | 0.7 | 2.6 | 74.9 | 0.7 | 3.4 | 78.2 | KH |

Table 2 Summary of aquifer hydraulic properties

| VES | $\rho_b (\Omega m)$ | $\rho_w (\Omega m)$ | F[] | Φ [] | τ [] | $K \times 10^{-5}$ [m/s] | h [m] | S (Ω^{-1}) | T (Ωm^2) | Tr [m ² /day] | K/ρ_b [Siemens/day] | Lithologic description of sandy units |
|-------|---------------------|---------------------|----------|-------------|-----------|--------------------------|-----------|---------------------|--------------------|--------------------------|--------------------------|---------------------------------------|
| 1 | 1945.6 | 109.3 | 17.8 | 0.102 | 1.35 | 0.58 | 68.1 | 0.035 | 132,495 | 34.261 | 0.000259 | Gravelly |
| 2 | 751.8 | 60.3 | 12.5 | 0.130 | 1.27 | 1.23 | 108.1 | 0.144 | 81,270 | 114.726 | 0.001412 | Medium |
| 3 | 2332.5 | 150.8 | 15.5 | 0.111 | 1.31 | 0.78 | 81.1 | 0.035 | 189,166 | 54.549 | 0.000288 | Gravelly |
| 4 | 735.5 | 68.5 | 10.7 | 0.142 | 1.23 | 1.71 | 87.7 | 0.119 | 64,503 | 129.942 | 0.002015 | Medium |
| 5 | 165.5 | 20 | 8.3 | 0.167 | 1.18 | 2.98 | 43.3 | 0.262 | 7166 | 111.616 | 0.015575 | Fine |
| 6 | 362.2 | 36.2 | 10.0 | 0.148 | 1.22 | 1.99 | 170.3 | 0.470 | 61,683 | 292.107 | 0.004736 | Fine |
| 7 | 187.8 | 15.6 | 12.0 | 0.132 | 1.26 | 1.34 | 110.5 | 0.588 | 20,752 | 127.966 | 0.006166 | Fine |
| 8 | 197.7 | 14 | 14.1 | 0.118 | 1.29 | 0.95 | 51.9 | 0.263 | 10,261 | 42.636 | 0.004155 | Fine |
| 9 | 1115.9 | 90 | 11.2 | 0.138 | 1.24 | 1.55 | 105.3 | 0.094 | 117,504 | 141.400 | 0.001203 | Medium |
| 10 | 203.8 | 16 | 12.7 | 0.127 | 1.27 | 1.19 | 30.9 | 0.152 | 6297 | 31.702 | 0.005034 | Fine |
| 11 | 396.7 | 34.5 | 11.5 | 0.135 | 1.25 | 1.47 | 5.4 | 0.014 | 2142 | 6.851 | 0.003198 | Fine |
| 12 | 549.2 | 52.3 | 10.5 | 0.144 | 1.23 | 1.79 | 47.8 | 0.087 | 26,252 | 73.769 | 0.00281 | Medium |
| 13 | 750.3 | 70.2 | 10.7 | 0.142 | 1.23 | 1.71 | 11.8 | 0.016 | 8854 | 17.484 | 0.001975 | Medium |
| 14 | 1721.4 | 109 | 15.8 | 0.110 | 1.32 | 0.75 | 55.2 | 0.032 | 95,021 | 35.659 | 0.000375 | Medium |
| 15 | 166.3 | 25.9 | 6.4 | 0.198 | 1.12 | 5.33 | 2.6 | 0.015 | 432 | 11.975 | 0.027695 | Fine |
| Mean | 772.1 | 58.2 | 12.0 | 0.136 | 1.25 | 1.69 | 65.33 | 0.156 | 54,920 | 81.776 | 0.005126 | |
| Range | 166.3–2332.5 | 14.0–150.8 | 6.4–17.8 | 0.102–0.198 | 1.12–1.35 | 0.748–5.33 | 2.6–170.3 | 0.016–0.588 | 432–61,683 | 6.851–292.107 | 0.000259–0.015575 | |

Table 3 Corrosivity rating of topsoil and protective strength of hydrogeological units

| VES no. | Resistivity of first layer (Ωm) | Weighted longitudinal conductance(Siemens) | Soil corrosivity rating | Groundwater protective rating |
|---------|---|--|-------------------------|-------------------------------|
| 1 | 120.0 | 1.137 | Slightly corrosive | Good |
| 2 | 206.8 | 0.601 | Non corrosive | Moderate |
| 3 | 873.2 | 1.143 | Non corrosive | Good |
| 4 | 1020.6 | 0.127 | Non corrosive | Weak |
| 5 | 71.8 | 0.037 | Slightly corrosive | Poor |
| 6 | 554.2 | 0.491 | Non corrosive | Moderate |
| 7 | 469.5 | 0.592 | Non corrosive | Moderate |
| 8 | 392.5 | 0.269 | Non corrosive | Moderate |
| 9 | 115.8 | 2.332 | Slightly corrosive | Good |
| 10 | 403.5 | 0.155 | Non corrosive | Weak |
| 11 | 90.5 | 3.760 | Slightly corrosive | Good |
| 12 | 660.4 | 0.043 | Non corrosive | Poor |
| 13 | 205.8 | 1.021 | Non corrosive | Good |
| 14 | 210.7 | 0.277 | Non corrosive | Moderate |
| 15 | 136.4 | 0.459 | Slightly corrosive | Moderate |

Despite the effort by organizations, waterborne diseases appear to subsist due to the use of brackish/saline water obtained from contaminated aquifer repositories (UNEP 2011). In spite of the huge amount of money made available by many donor agencies, the dwellers prefer hand-dug boreholes which are cheap and very shallow to motorized boreholes which are somewhat expensive and safe. Particularly, during the dry seasons when the water is highly brownish from the boreholes, desperation compels the people living and doing business in this area to resort to sourcing for water from the Imo River, the brackish and dependable surface water in the area. After consultancy services involving hydrogeological and geophysical investigations and analyses of results, this report of groundwater parameters and freshwater–saltwater interface in ALSCON and its adjoining areas is presented. It is expected that our findings which include characterization, spatial distribution of the main hydrological units, groundwater potential, recharge and flow pattern will be found useful in groundwater management in the area and other places with similar geologic settings and problems.

Location and geology of the study area

Physiographically, the study area shown in Fig. 1 lies between longitudes 7° 30' E and 7° 35' E and latitudes 4° 30' N and 4° 35' N in Ikot Abasi local government area (Aluminium town) of Akwa Ibom State in the

Niger Delta region of southern Nigeria. The study area is bordered by Oruk Anam local government area (L.G.A) in the north, Mkpato Enin L.G.A in the west, and the Eastern Obolo L.G.A and the Atlantic Ocean in the south. The Imo River forms the natural boundary in the east separating it from Rivers State (Fig. 1). Ikot Abasi covers an area of approximately 451.73 sq. km. The study was designed to cover Ikpa Ibekwe Clan in Ikot Abasi local government area of Akwa Ibom State of Nigeria, where ALSON is located. The choice is unique as this part is densely populated with people who extract groundwater for drinking and domestic usages.

The study area is located in an equatorial climatic region that is characterized by two major seasons. The seasons are the rainy season (March–October) and dry season (November–February) (Aristodemou and Thomas-Betts 2000; George et al. 2010). The dry

Table 4 Modified longitudinal conductance/protective capacity rating (Henriet 1976; Oladapo et al. 2004; George et al. 2014b)

| Longitudinal conductance (mhos) | Protective capacity rating |
|---------------------------------|----------------------------|
| 10 | Excellent |
| 5–10 | Very Good |
| 0.7–4.9 | Good |
| 0.2–0.69 | Moderate |
| 0.1–0.19 | Weak |
| 0.1 | Poor |

Table 5 Classification of soil resistivity in terms of corrosivity (Oladapo et al. 2004)

| Soil Resistivity (Ωm) | Soil corrosivity |
|---------------------------------|---------------------------|
| <10 | Very strongly corrosive |
| 10–60 | Moderately corrosive |
| 60–180 | Slightly corrosive |
| 180 \geq | Practically non-corrosive |

season is a period of extreme aridity characterized by excruciating high temperatures that do reach 35 °C. The area has been severely affected by the current global climatic changes in such a way that there have been shifts in both the upper and lower boundaries of these climatic conditions (Martínez et al. 2008; Rapti-Caputo 2010; Riddell et al. 2010; Wagner and Zeckhauser 2011; Farauta, et al. 2012)

Geologically, the study area is located in the Tertiary to Quaternary Coastal Plain Sands (CPS) (otherwise called the Benin Formation) and Alluvium environments of the Niger Delta region of southern Nigeria (Fig. 1). The Benin Formation which is underlain by the Paralic Agbada Formation covers over 80 % of the study area. The sediments of the Benin Formation consist of interfringing units of lacustrine and fluvial loose sands, pebbles, clays, and lignite streaks of varying thicknesses while the alluvial units comprise tidal and lagoonal sediments, beach sands, and soils (Reijers et al. 1997; Nganje et al. 2007) which are mostly found in the

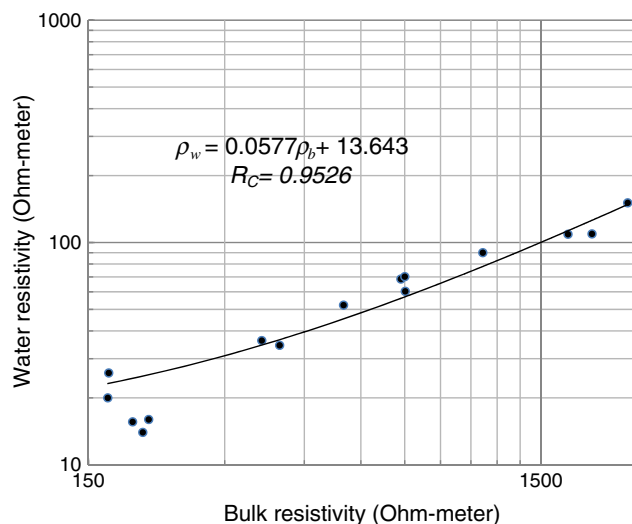


Fig. 4 A graph of aquifer water resistivity against bulk resistivity

southern parts and along the river banks. The CPS is covered by thin lateritic overburden materials with varying thicknesses at some locations but is massively exposed near the shorelines. The CPS forms the major hydrogeologic units in the area. It comprises poorly sorted continental (fine–medium–coarse) sands and gravels that alternate with lignite streaks, thin clay horizons, and lenses at some locations. The thin clay/shale horizons truncate the vertical and lateral extents of the sandy aquifers thereby building up multiaquifer systems in the area (Evans et al. 2010; George et al. 2010, 2014b). Thus, both confined and semiconfined aquifers

Fig. 3 Map showing the distribution of elevation (m) above mean sea level in the study area

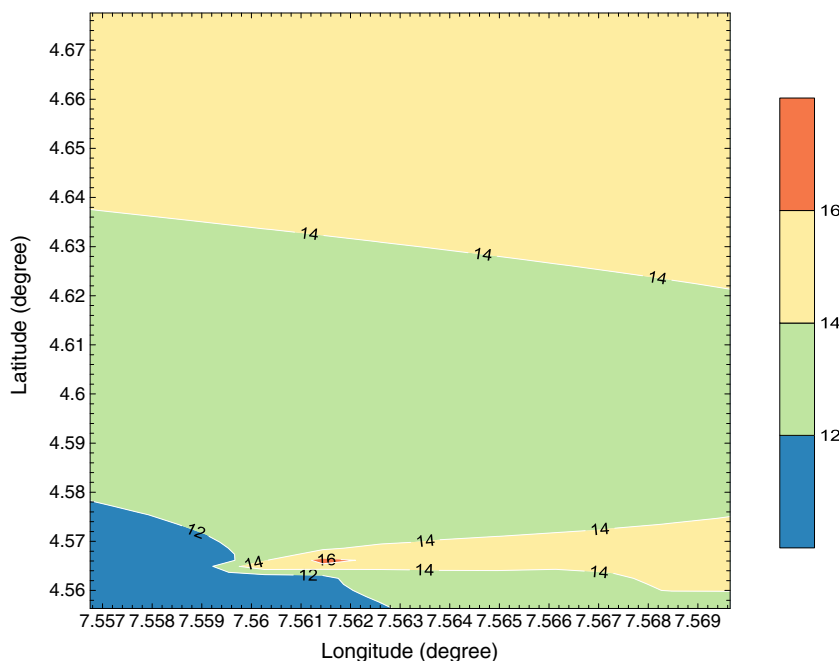
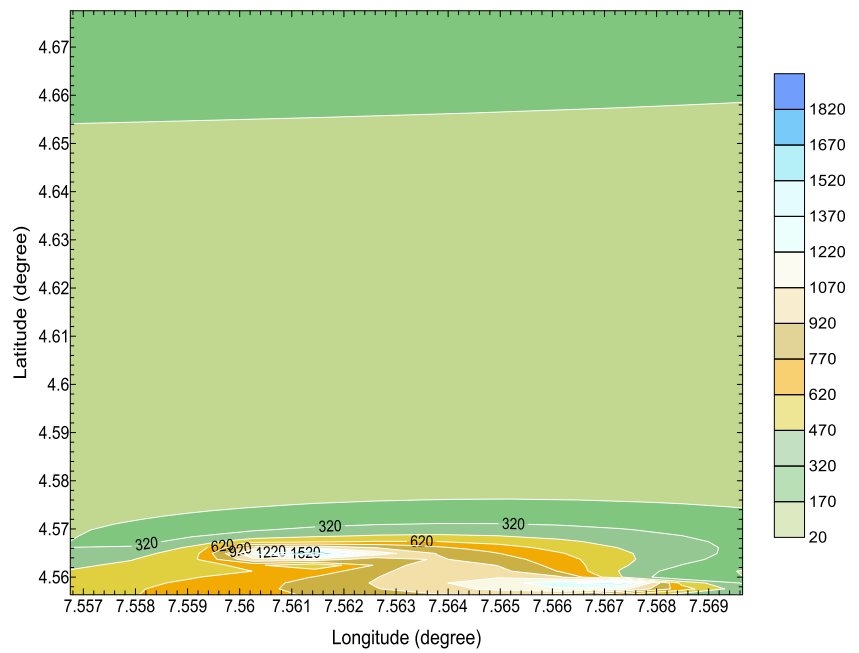


Fig. 5 Map showing aquifer bulk resistivity (Ωm) distribution in the study



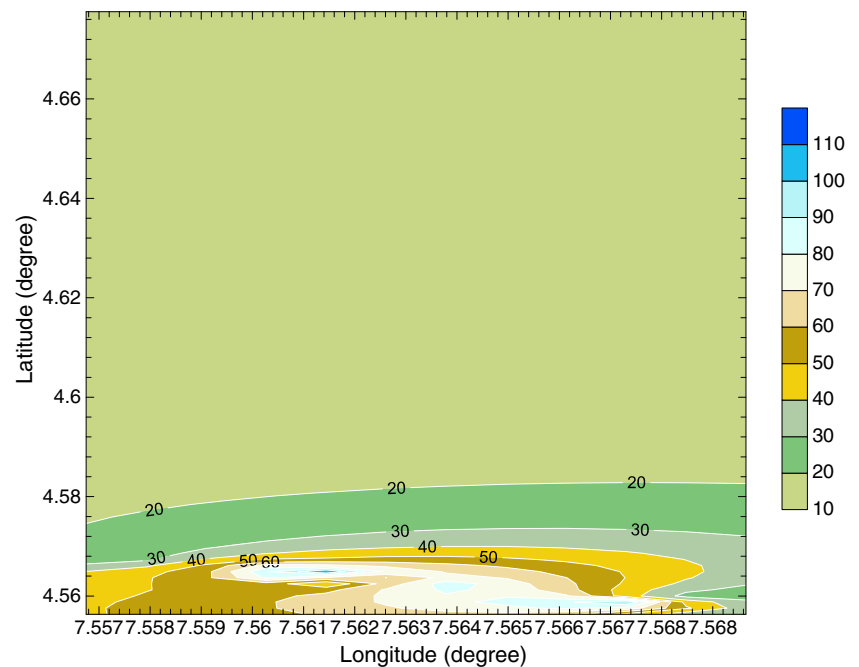
can be found in the area whose static water level (SWL) ranges from 1.7 to 14.7 m.

The area is drained by southward flowing rivers such as the Imo River and their tributaries that empty directly into the Bight of Bonny (George et al. 2011b). The brackish/saline water in Imo River interacts with the freshwater aquifers through the geologic divides thereby causing serious health threats to lives. This provokes the choice of this case study in the region characterized with high population density.

Materials and methods

In this study, 15 VES were conducted in the study area (Fig. 1) with a maximum current electrode half spacing (AB/2) of 400 to 500 m. Digital signal averaging system (SAS) (1000 ABEM Terrameter) was used for acquiring the resistivity data. Though there are several abandoned corrosive groundwater boreholes reflected by the overflow of brownish water/saline water, all the VES stations in this study were conducted near existing

Fig. 6 Map showing aquifer water resistivity (Ωm) distribution in the study area



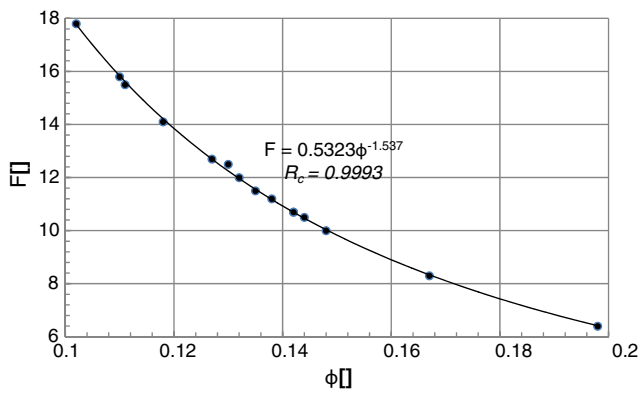


Fig. 7 A graph of aquifer resistivity formation factor against fractional porosity

functional water boreholes. Therefore, 15 water samples were collected from the respective boreholes for estimation of water resistivity (ρ_w). In the water samples, in situ measurements of electrical conductivity were performed in all the boreholes using a WTW LF91 conductivity meter and the resistivity of water was inferred from water conductivity.

Two of the VES stations (VES 12 and VES 15) were sited near the ALSCON head office where pump tests were performed after drilling the boreholes for comparison of hydraulic conductivity obtained with the one obtained from VES data. In conducting the pump test, the fall in water level with respect to time was measured and the interpretation was done using Jacob straight-line method according to Fetters (1994). The

inferred hydraulic conductivities from pump tests were 8.10×10^{-5} m/s (0.69 m/day) for borehole near VES station 12 and 5.78×10^{-5} m/s (4.99 m/day) for borehole near VES station 15.

The apparent resistivity (ρ_a) estimated from calculated geometric factor and the measured resistance according to the expression were inverted to true geological models using WINRESIST, a 1D inversion software package.

To ensure fidelity in the measurements, all depths were constrained by nearby water borehole information in which example is shown in Fig. 2. The model geoelectric parameters (depth, thickness, and resistivity) for all VES in all the stations were employed in estimating parameters shown in Table 1. The fractional porosity of the Quaternary alluvial sands of hydrogeological units was estimated using Archie's law (Archie 1942) which relates geoelectric parameters to hydraulic parameters using the expression in Eq. 1:

$$\frac{\rho_b}{\rho_w} = F = \frac{a}{\phi^m} \tag{1}$$

where ρ_b , ρ_w , F , a , m , and ϕ are bulk resistivity, water resistivity, resistivity formation factor, pore geometry factor, cementation factor, and fractional porosity, respectively. The average values of $a=0.5245$ and $m=1.5431$ estimated in the region for similar geologic materials (George et al. 2011a, 2015a) were used in the above expression. The tortuosity (the ratio of dis-

Fig. 8 Map showing distribution of aquifer resistivity formation factor in the study area

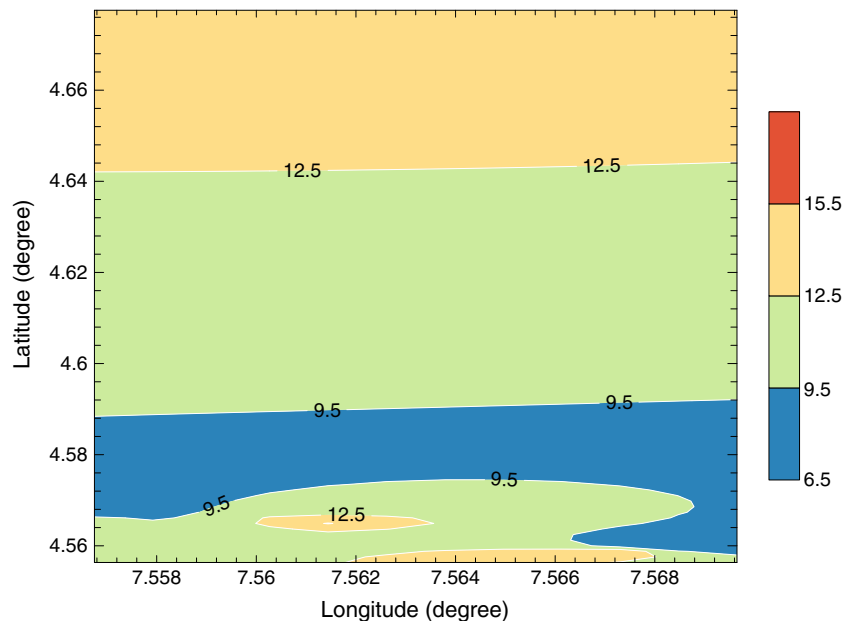
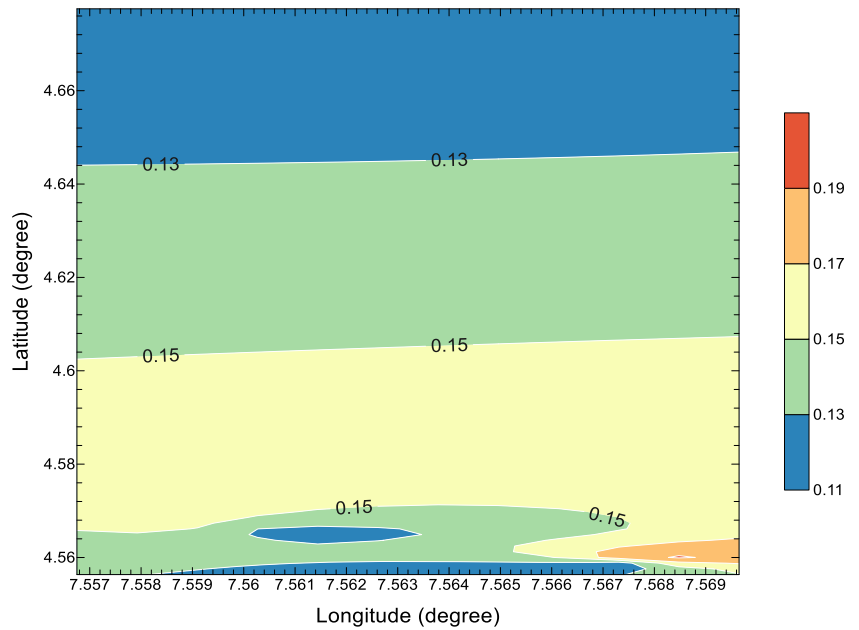


Fig. 9 Map showing distribution of aquifer fractional porosity in the study area



tance actually travelled by the fluid through the porous media to the macroscopic length (straight line from the inlet face to the outlet face)) was computed using the expression in Eq. 2:

$$\tau = (F \cdot \phi)^{\frac{1}{2}} \tag{2}$$

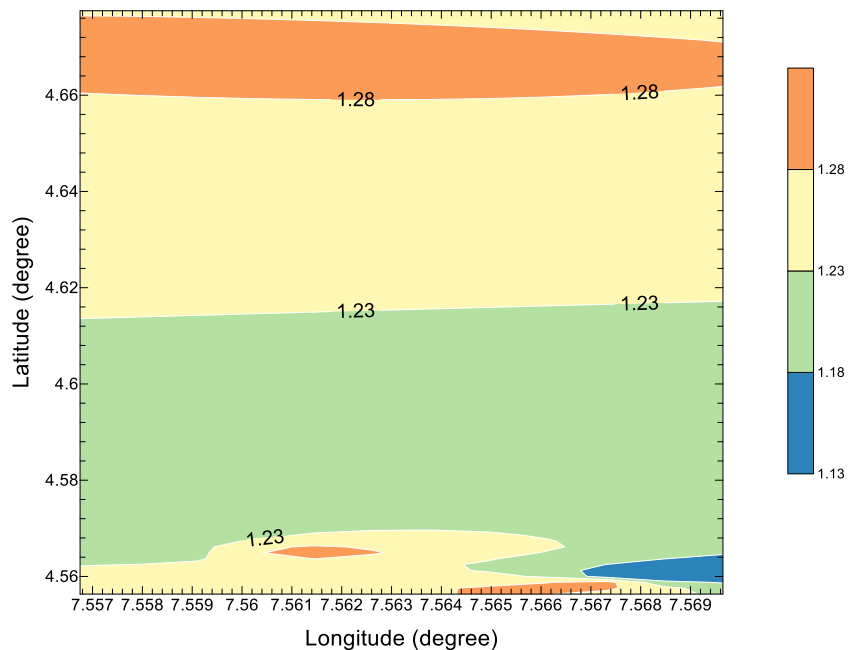
Using the Kozeny–Carman–Bear’s Model (KCBM) equation which establishes a quantitative relationship between hy-

draulic conductivity K with porosity ϕ and other site-dependent parameters, in the expression below, the hydraulic conductivities for the different VES locations were estimated using Eq. 3:

$$k \approx \left(\frac{\delta_w g}{\mu_d} \right) \cdot \left(\frac{d_m^2}{180} \right) \cdot \left[\frac{\phi^3}{(1-\phi)^2} \right] \tag{3}$$

where δ_w is the density of water (taken as 1000 kg/m^3), d_m is the mean grain size of sediments which was determined in

Fig. 10 Map showing distribution of aquifer tortuosity in the study area



this study by direct measurement using Vernier Callipers and micrometer screw gauge to be 0.000348 m and μ_d is the dynamic viscosity of water which according to Fetters (1994) can be taken to be 0.0014 kg/ms for fine–coarse sands. Estimated K , h , ρ_b , and F for the safe hydrologic units in Table 2 were used to estimate the Dar Zarouk parameters (longitudinal conductance S ($\frac{h}{\rho}$) and transverse resistance T (ρh); tortuosity τ ($F\phi$)^{1/2}; transmissivity Tr (Kh) and the electrical conductivity–hydraulic conductivity productivity of the aquifer units. The protective strength of each of the economic saturated hydrological units was evaluated in Table 3 in conjunction with Table 4 using the weighted longitudinal conductance, according to the expression in Eq. 4:

$$\alpha = \sum_{i=1}^n \frac{h_i}{\rho_i} \tag{4}$$

Where ρ_i is the true resistivity of each layer and h_i the saturated thickness of each layer. The corrosivity of the soil suspected to have been existed due to the past and recent operations of the ALSCON was also evaluated in Table 3 using the resistivity value of the first layer on each VES station in the study area by comparing with the corrosivity rating in Table 5.

Results and discussion

The analysis of the geoelectric survey reveals three to four geoelectric layers with characteristic different curve types indicated in Table 1 within the study area. Measurements from GPS radar indicate the area is low-lying with the elevation ranging from 10–20 m with an average value of 13.47 m. The distribution of elevation is shown in Fig. 3. The elevation decreases from north to the south and further shows a sharp increase in a southeast–southwest trend (Fig. 3). This indicates that groundwater flows from north to south and finally empties into the Imo River in the southwestern part of the study area on the average. From the VES curves or the interpreted results in Table 1, some layers show large thicknesses with remarkably reduced resistivity ranging from 8.2 Ωm (94.5 m thick) in VES 11 to 71.3 Ωm (81.1 m thick) in VES 3. The zones of remarkable reduction or inversion in layer resistivity values serve as possible points of interaction between freshwater and saltwater. The topmost layers have thicknesses

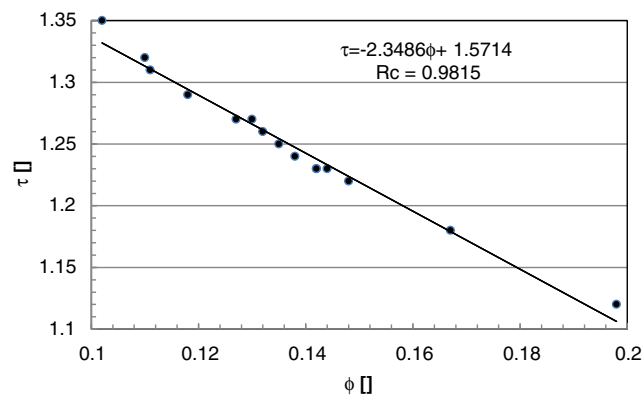


Fig. 11 A graph of aquifer tortuosity against fractional porosity

ranging from 0.5 m (VES 5) to 11.3 m (VES 6) with an average of 3.07 m. The topmost layer also has varying values of resistivities (71.8–1020.6 Ωm ; average 368.78 Ωm). The resistivity of economic hydrogeologic units ranged from 166.3 Ωm to 2332.5 Ωm with an average value of 772.1 Ωm . This is an indication that the economic hydrogeologic units in the area have bulk resistivity values greater than 100 Ωm for uncontaminated fine to coarse sands (Hinnell et al. 2010). The water resistivity of hydrogeologic units also displayed range from 14.0 to 150.8 Ωm and average value of 58.2 Ωm . A plot of water resistivity versus bulk resistivity shows a proportional increase (Fig. 4) with diagnostic expression with high correlation coefficient ($R_c = 0.95$) given in Eq. 5;

$$\rho_w = 0.0577\rho_b + 13.643 \tag{5}$$

The distribution of bulk water resistivity and water resistivity are displayed in Figs. 5 and 6, respectively.

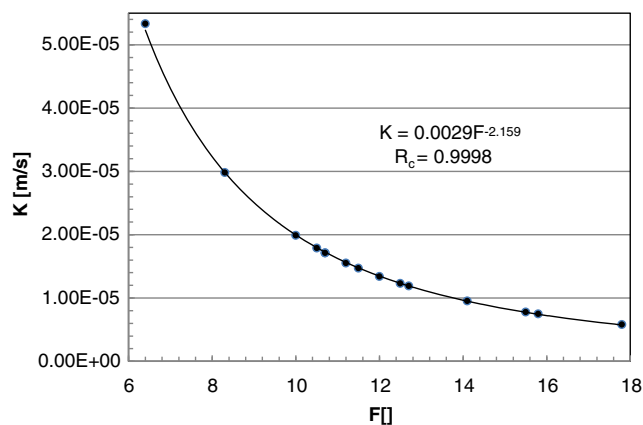


Fig. 12 A graph of aquifer hydraulic conductivity against resistivity formation factor

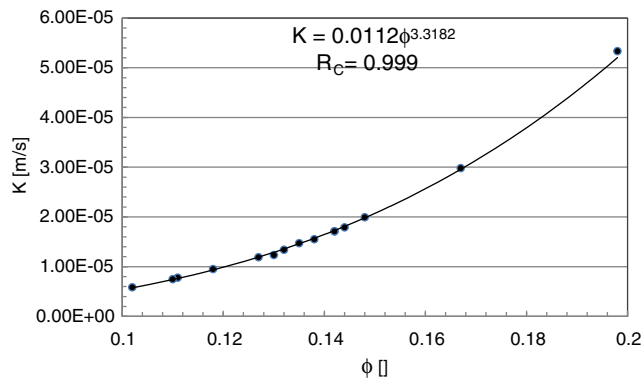
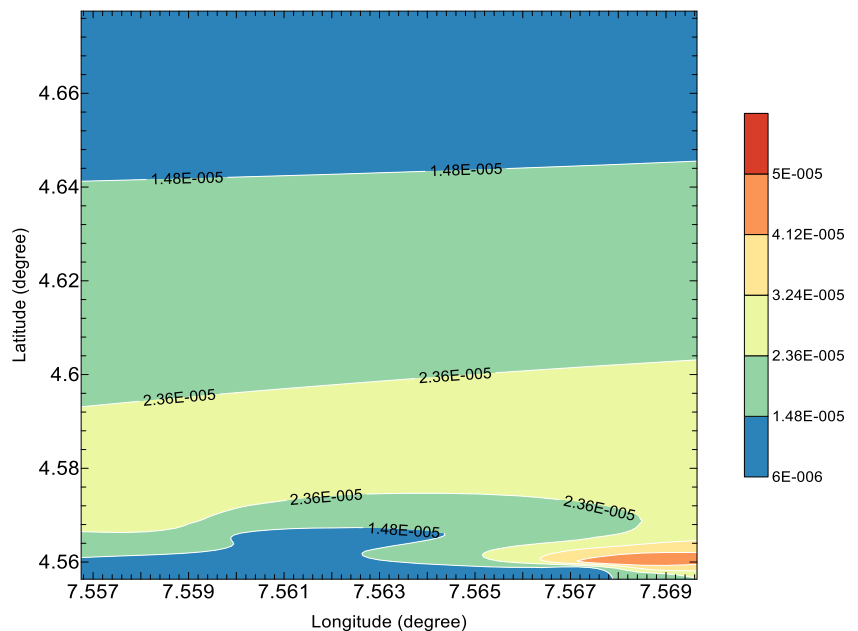


Fig. 13 A graph of aquifer hydraulic conductivity against fractional porosity

In Figs. 5 and 6, high bulk resistivity and water resistivity are seen in the southern part of the study area while moderately low values are distributed on other parts of the study area. The reason for this distribution may be due to the natural geological formation composition and divide (Mbonu et al. 1991). This clearly indicates that in the southern region of the study area, the hydrological units are protected from being exposed to interaction with the brackish water for borehole depths greater than 40 m due to hydrogeological formation divide. However, the conductivity of water increases (the resistivity decreases) toward the north due to divides between formations and geological formations in the study area (Mauro et al. 2014).

Fig. 14 Map showing distribution of aquifer hydraulic conductivity (m/s) in the study area



Based on the bulk resistivity and water resistivity values, the computed resistivity formation factor ranged from 6.4–17.8 with an average of 12.0 were plotted with fractional porosity ranging from 0.102–0.198 with average value of 0.136 in Fig. 7. The plot shows an inverse diagnostic power function with high correlation coefficient ($R_c=0.999$) given in Eq. 6:

$$F = 0.5323\phi^{-1.537} \tag{6}$$

The power (1.537) and the coefficient of ϕ (0.5323) represent the average cementation factor (m) and pore geometry factor (a) of the hydrogeological units respectively. These diagnostic constants can be used to estimate fractional porosity in other zones with similar geologic formations once bulk and water resistivities are available. The distributions of resistivity formation factor, fractional porosity, and tortuosity are shown in Figs. 8, 9, and 10. From Fig. 8, resistivity formation factor are gradually higher in the north and some points in the south with an inversion in between north and south of the study area. It can be inferred from Fig. 9 that porosity increases inversely with resistivity formation factor. Hence, higher values are seen on the south where resistivity formation factor is lower in accordance with $F-\phi$ relation in Eq. 6. Again, the tortuosity shows an inverse relation in both Figs. 10 and 11 with porosity and proportional increase relation with resistivity formation factor. The $\tau-\phi$ relation in Fig. 11 and the highly correlated diagnostic characteristic expression in

Eq. 7 can be used in place of Eq. 2 to estimate tortuosity in the study area.

$$\tau = -2.3466\phi + 1.5714 \tag{7}$$

Figure 10 portrays that groundwater flow speed is reduced in the southern region of the study area where the porosity is higher. This could be caused by poor communication between pores in the flow channel. The relationship between hydraulic conductivity and resistivity formation factor also shows inverse relation in Fig. 12 with diagnostic equation characterized by high correlation coefficient ($R_c=0.999$) in the expression of Eq. 8:

$$K = 0.0029F^{-2.159} \tag{8}$$

Just as porosity is proportional to coefficient of permeability (hydraulic conductivity), as indicated in Fig. 13 and a highly correlated diagnostic expression in Eq. 9, resistivity

$$K = 0.0112\phi^{3.3182} \tag{9}$$

Formation factor of hydrogeological units is inversely related with hydraulic conductivity. Hence, higher hydraulic conductivity in the southern region of the study area further proves that hydrogeological formations with high porosity would likely characterize the south than the north of the study area though some portions of the south reflect some low values of hydraulic conductivities in Fig. 14. The estimated thick-

Fig. 15 **a** Map showing distribution of aquifer thickness (m) in the study area. **b** A graph of aquifer formation factor against aquifer thickness

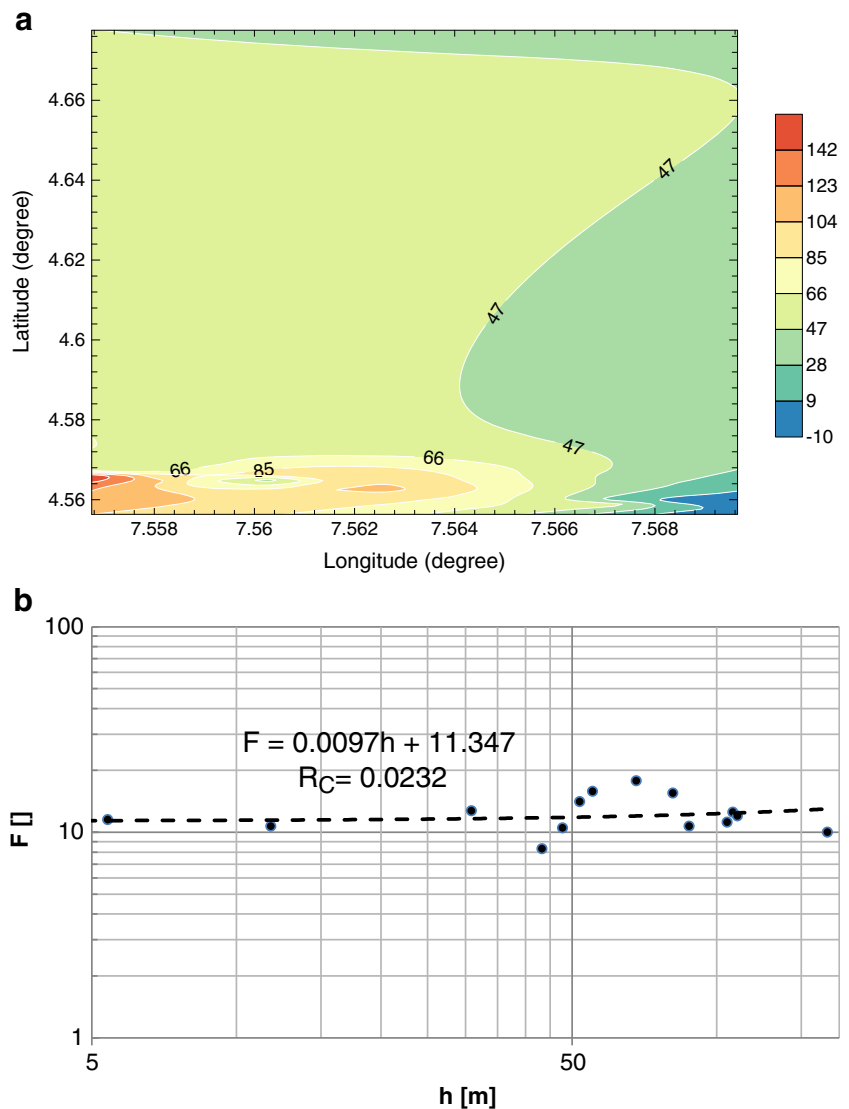
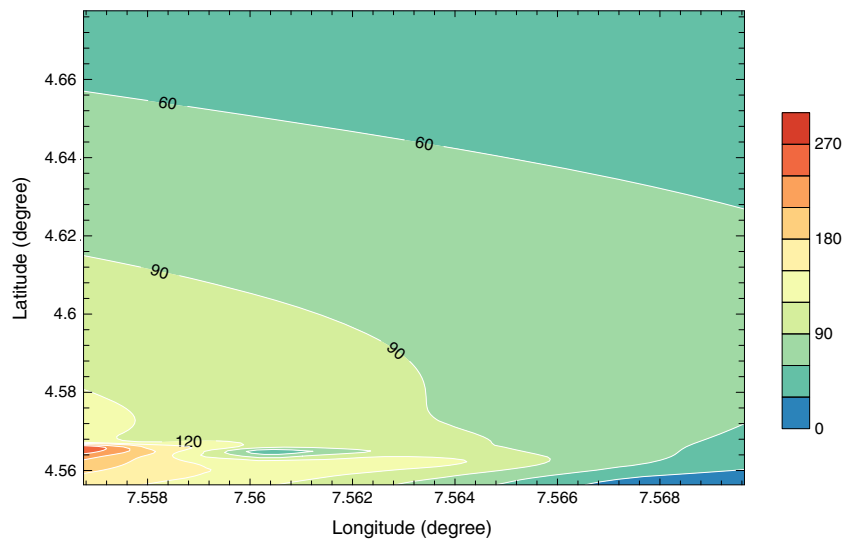


Fig. 16 Map showing distribution of aquifer transmissivity (m^2/day) in the study area



nesses of aquifer units showing higher values in the western part and lower values in the northeast–south-east trending in Fig. 15a indicate non-correlated fairly constant relationship with resistivity formation factor in Fig. 15b. The $F-h$ relation in Fig. 15b gives the governing equation with weak correlation ($R_c=0.0323$) in Eq. 10:

$$F = 0.0097h + 11.34 \tag{10}$$

The poor correlation coefficient could be attributed to the varying grain size of hydrogeological units in the study area. The equation indicates that for various

thicknesses of aquifer units, resistivity formation factor remains unchanged at its average value given by the intercept of the $F-h$ relation, in a system of hydrogeological units.

The transmissivities (T_r) of the hydrogeological units were also computed as shown in Table 2 through the $K-h$ products in m^2/day , and their distribution in the study area is displayed in Fig. 16. The trend shows that Transmissivity increases in a north-east–southwest direction. The higher transmissivity in the southwestern portion of the study area is an indication of the high groundwater reserve in the southwest than in other parts of the area under investigation.

The $K-\rho_b$ ratio in Siemens/day with transverse resistance plot in Fig. 17 indicates an inverse relation with a good correlated equation ($R_c=0.642$) in expression given in Eq. 11:

$$K/\rho_b = 1.2546T_r^{-0.625} \tag{11}$$

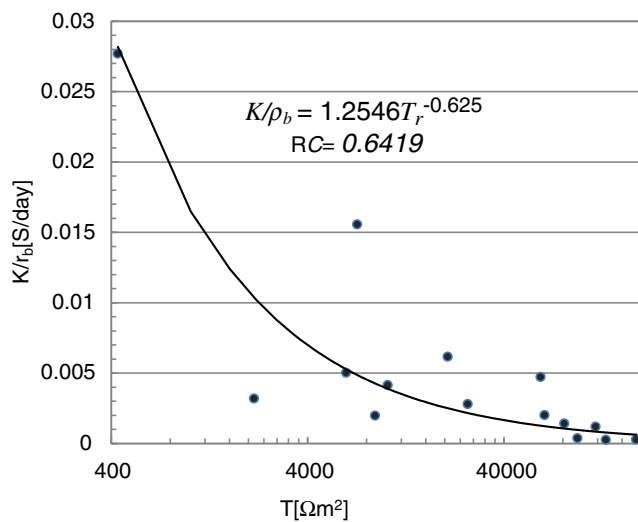
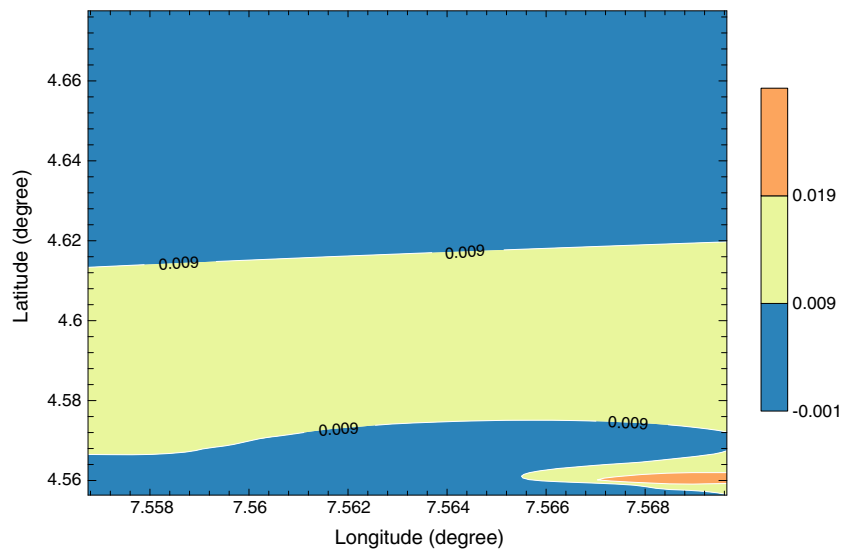


Fig. 17 A graph of aquifer ratio of hydraulic conductivity to bulk water resistivity against transverse resistance

Although some scattered points believed to have been due to anisotropy and varying grain size are noticed in the plot, transverse resistance decreases with increasing $K-\rho_b$ ratio and the diagnostic equation above can be used to estimate the rate of fall of electrical conductance in an aquifer unit for a given area of electrical conductance of an aquifer. The $K-\rho_b$ ratio map in Fig. 18 compares with hydraulic conductivity map in Fig. 14. The analogy in the variation indicates that the rate of electrical conductance of an aquifer unit increases with the coefficient of permeability (George et al. 2015a). Hence, where hydraulic conductivity is

Fig. 18 Map showing distribution of aquifer rate of conductance (Siemens per day) in the study area



high, the rate of electrical conductance is also high. The longitudinal conductance in Table 2 shows lower values generally. This is an indication of vulnerability of the aquifer to contamination. The spread of longitudinal conductance in Fig. 19 shows that the southern region characterized with higher pollution of groundwater reserve is more vulnerable to surface contamination than the northern region of the study area.

The protective strength of hydrogeological units and soil corrosivity in the study area were evaluated as shown in Table 3. As summarized on the table, aquifers in VES 5 and 12 have poor protective strength while aquifers in VES 4 and 10 have weak protective strength based on their weighted longitudinal

conductance. Aquifers in other VES stations have their protective strength ranging from moderate to good protective strengths. The soil showed non-corrosivity except in five VES stations covering VES 1, 5, 9, 11, and 15 in which the soil is slightly corrosive. In VES 5 station, the topsoil is corrosive and the aquifer unit has poor protective strength which is attributable to the corrosion of metal, rubber tank, and the raised concrete platform used for carrying the borehole water tank located near the VES in Fig. 20. This problem is not limited to aquifer in VES 5 station alone, it is also responsible for groundwater pollutions associated with corrosion or rusting of water tanks in other places in the region

Fig. 19 Map showing distribution of aquifer longitudinal conductance (Siemens) in the study area

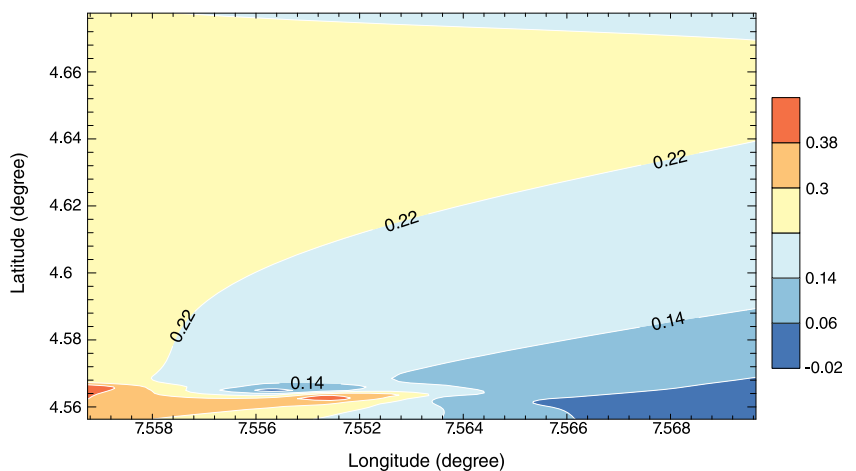




Fig. 20 A picture showing a typical abandoned borehole with corroded rubber tank, raised concrete platform, and plastic pipes due to contamination of aquifer near VES 5

Conclusion

The integrated study presented in this work demonstrates that the combined use of geoelectrical and laboratory techniques can provide a useful tool for monitoring, modeling, and managing groundwater contamination. These tools can prove extremely useful in estimating geohydrodynamic parameters such as porosity and hydraulic parameters, which are paramount in assessing the flow of contaminants in groundwater repositories mostly in area where limited information from boreholes exist. The porosity values and other hydraulic parameters estimated from inexpensive geophysical method correlated fairly well with the values obtained from the conventional methods and have proved that the study area has unprotected overburden layers. Thus, the use of pumping test data from limited data and geophysical method in this work serves as useful pair in economical and quantitative estimation of aquifer parameters and diagnosis of groundwater problems associated with pollution or corrosion. The estimation of porosity and hydraulic conductivity for the area assisted in the estimation of transmissivity and tortuosity, which by their estimated values confirm the prolific nature of groundwater repositories in the area. Although increase in porosity and hydraulic conductivity do not necessarily translate to increase in pore water, the findings through various diagnostic equations and spatial distribution of parameters displayed on maps are valuable tools for groundwater flow modeling studies. Empirical relationships connecting porosity and other hydraulic parameters of a saturated formation have been generated. The ranges of experimentally estimated hydraulic parameters and the earth system diagnostic equations derived using regression analysis could be used to estimate the input parameters for contaminant migration modeling and also to improve on the quality of existing models. Since porosity and permeability are important parameters in oil exploration/exploitation in which the area is known for, the models realized in this study will also be considered as input parameters during well development. The results show that the aquifers are highly

vulnerable to contamination from the various sources of contamination including hydrocarbon that abounds. Although the weighted longitudinal conductance in a few locations are greater than unity and some of the top soils evaluated are non-corrosive, there are needs for closer monitoring of the hydrogeological units in the area where oil spills, industrial pollutants, and other adverse effects of oil exploration and exploitation activities are the trade-off between corrosion and pollution in surface and groundwater resources. The CPS of the Niger Delta region of Nigeria in which the study area is located is a fairly homogeneous geologic formation in terms of spatial spread of the various lithostratigraphic units, groundwater dynamics, and quality variations. Consequently, it is expected that the findings made in the present case study will not change significantly in the other locations except where the groundwater quality is seriously degraded by industry-related activities such as uncontrolled waste disposal, oil spills, and other hydrocarbon exploration and exploitation-related environmental problems. The findings will be veritably useful in the siting of exploratory boreholes and planning for appropriate prevention and remediation strategies for groundwater and other contaminated sites within the region where hydrocarbon exploration and exploitation activities have caused serious surface and subsurface contaminations.

Acknowledgments The authors are grateful to Akwa Ibom State University that provided the resources, which made this study successful. The manpower support and contributions by the community in which the work was carried out are also gratefully acknowledged. We particularly acknowledge the managing editor and the anonymous reviewers for their critical comments and suggestions which have improved the quality of the original manuscript.

References

- Akpan AE, Ugbaja AN, George NJ (2013) Integrated geophysical, geochemical and hydrogeological investigation of shallow groundwater resources in parts of the Ikom-Mamfe Embayment and the adjoining areas in Cross River State. *Nigeria Environ Earth Sci* 70(3):1435–1456. doi:10.1007/s12665-0132232-3
- Archie GE (1942) The electrical resistivity log as an aid in determining some reservoir characteristics. *Trans Am Inst Min Metall Pet Eng* 146:54–62
- Aristodemou E, Thomas-Betts A (2000) DC resistivity and induced polarisation investigations at a waste disposal site and its environments. *J Appl Geophys* 44:275–302
- Ekwe AC, Onu NN, Onuoha KM (2006) Estimation of aquifer hydraulic characteristics from electrical sounding data: the case of middle Imo River basin aquifers, south-eastern Nigeria. *J Spat Hydrol* 6(2):121–132
- Evans UF, George NJ, Akpan AE, Obot IB, Ikot AN (2010) A study of superficial sediments and aquifers in parts of Uyo local government area, Akwa Ibom State, Southern Nigeria, using electrical sounding method. *E-J Chem* 7(3):1018–1022

- Farauta BK, Egbule CL, Agwu AE, Idrisa YL, Onyekuru NA (2012) Farmers' adaptation initiatives to the impact of climate change on agriculture in northern Nigeria. *J Agric Ext* 16:132–144. doi:10.4314/jae.v16i1.13
- Fetters CW (1994) *Applied hydrogeology*, 3rd edn. Prentice Hall Inc., New Jersey, p 600
- George NJ, Akpan AE, Obot IB (2010) Resistivity study of shallow aquifer in parts of southern Ukanafun local government area, Akwa Ibom state. *E- J Chem* 7(3):693–700
- George NJ, Obianwu VI, Obot IB (2011a) Estimation of groundwater reserve in unconfined frequently exploited depth of aquifer using a combined surficial geophysical and laboratory techniques in the Niger delta, southern Nigeria. *Adv Appl Sci Res, Pelegia Res Libr* 2(1):163–177
- George NJ, Obianwu VI, Udofia KM (2011b) Estimation of distribution of aquifer parameters in the southern part of Akwa Ibom state, southern Nigeria using surficial geophysical measurements. *Int Rev Phys, Praise Worthy Prize, Italy* 5(2):53–59
- George NJ, Akpan AO, Umoh AA (2013) Preliminary geophysical investigation to delineate the groundwater conductive zones in the coastal region of Akwa Ibom state, southern Nigeria, around the Gulf of Guinea. *Int J Geosci* 4:108–115. doi:10.4236/ijg.2013.4101
- George NJ, Ubom AI, Ibanga JI (2014a) Integrated approach to investigate the effect of leachate on groundwater around the Ikot Ekpene Dumpsite in Akwa Ibom State, South-eastern Nigeria. *Int J Geophys, Hindawi Publ Com* 2014:1–10. doi:10.1155/2014/174589
- George NJ, Ekong UN, Etuk SE (2014b) Assessment of economically accessible groundwater reserve and its protective capacity in eastern obolo local government area of Akwa Ibom state, Nigeria, using electrical resistivity method, international journal of geophysics. *Hindawi Publ Com* 2014:1–10. doi:10.1155/2014/578981
- George NJ, Emah JB, Ekong UN (2015a) Geohydrodynamic properties of hydrogeological units in parts of Niger Delta, southern Nigeria. *J Afr Earth Sci* 105:55–63. doi:10.1016/j.jafrearsci.2015.02.009
- George NJ, Ibanga JI, Ubom AI (2015b) Geoelectrohydrogeological indices of evidence of ingress of saline water into freshwater in parts of coastal aquifers of Ikot Abasi, southern Nigeria. *J Afr Earth Sci* 109:37–46. doi:10.1016/j.jafrearsci.2015.05.001
- Henriet JP (1976) Direct application of Dar- Zarrouk parameters in groundwater survey. *Geophys Prospect* 24:344–353
- Hinnell AC, FerréTPA, Vrugt JA, Huisman JA, Moysey S, Rings J, Kowalsky MB (2010) Improved extraction of hydrologic information from geophysical data through coupled hydrogeophysical inversion. *Water Resources Research* 46, W00D40, doi:10.1029/2008WR007060
- Ibuot JC, Akpabio GT, George NJ (2013) A survey of the repository of groundwater potential and distribution using geoelectrical resistivity method in Itu local government area (L.G.A), Akwa Ibom state, southern Nigeria. *Cent Eur J Geosci* 5(4):538–547. doi:10.2478/s13533-012-0152-5
- Keswick BH, Wang D, Gerba CP (1982) The use of micro-organisms as groundwater tracers—a review. *Groundwater* 20(2):142–149
- Martínez AG, Takahashi K, Núñez E, Silva Y, Trasmonte G, Mosquera K, Lagos P (2008) A multi-institutional and interdisciplinary approach to the assessment of vulnerability and adaptation to climate change in the Peruvian Central Andes: problems and prospects. *Adv Geosci J* 14:257–260
- Mauro M, Silvia I, Mauro G, Riccardo B (2014) Relating electrical conductivity of alluvial sediments to textural properties and pore-fluid conductivity. *Geophys Prospect* 62(3):1–15. doi:10.1111/1365-2478.12102
- Mbonu DDC, Ebeniro JO, Ofoegbu CO, Ekine AS (1991) Geoelectrical sounding for the determination of aquifer characteristics in parts of the Umuahia area of Nigeria. *Geophysics* 56(5):284–291
- Nganje TN, Edet AE, Ekwere SJ (2007) Concentrations of heavy metals and hydrocarbons in groundwater near petrol stations and mechanic workshops in Calabar metropolis, southeastern Nigeria. *J Environ Geosci* 14(1):15–29. doi:10.1306/eg.08230505005
- Obianwu VI, George NJ, Okiwelu AA (2011) Preliminary geophysical deductions of lithological and hydrological conditions of the north-eastern sector of Akwa Ibom state, south eastern Nigeria. *Res J Appl Sci, Eng Technol, Maxwell Sci Organ* 3(8):806–811
- Obinawu VI, George NJ, Udofia KM (2011) Estimation of aquifer hydraulic conductivity and effective porosity distributions using laboratory measurements on core samples in the Niger Delta, southern Nigeria. *Int Rev Phys, Praise Worthy Prize, Italy* 5(1):19–24
- Oladapo MI, Mohammed MZ, Adeoye OO, Adetola OO (2004) Geoelectric investigation of the Ondo State Housing Corporation Estate; Ijapo, Akure, Southwestern Nigeria. *J Min Geol* 40(1):41–48
- Rapti-Caputo D (2010) Influence of climatic changes and human activities on the salinization process of coastal aquifer systems. *Itaian J Agron River Agron* 3:67–79
- Reijers TJA, Peters SW, Nwajide CS (1997) The Niger Delta Basin. In: Selley RC (ed) *African basins—sedimentary basin of the world* 3. Elsevier Science, Amsterdam, pp 151–172
- Riddell ES, Lorentz SA, Kotze DC (2010) A geophysical analysis of hydro-geomorphic controls within a headwater wetland in a granitic landscape, through ERI and IP. *J Hydrol Earth Syst Sci* 14:1697–1713. doi:10.5194/hess-14-1697-2010
- Soupios PM, Kouli M, Vallianatos F, Vafidis A, Stavroulakis G (2007) Estimation of aquifer hydraulic parameters from surficial geophysical methods: a case study of Keritis Basin in Chania (Crete–Greece). *J Hydrol* 338:122–131. doi:10.1016/j.jhydrol.2007.02.028
- United Nations Environmental Programme, UNEP, (2011). *Environmental assessment of Ogoniland*. UNEP Publication. Exec Summa 3
- Wagner G, Zeckhauser RJ (2011) Climate policy: hard problem, soft thinking. *Clim Chang*. doi:10.1007/s10584-011-0067-z